ELSEVIER

Journal of Chromatography A, 827 (1998) 197–213

JOURNAL OF CHROMATOGRAPHY A

Network modeling of the intraparticle convection and diffusion of molecules in porous particles packed in a chromatographic column

J.J. Meyers, A.I. Liapis*

Department of Chemical Engineering and Biochemical Processing Institute, University of Missouri-Rolla, Rolla, MO 65409-1230, USA

Abstract

A pore network model (cubic lattice network) is constructed to represent the porous structure in a column packed with porous chromatographic particles. Expressions are developed and used to determine, through the utilization of the pore network model, the intraparticle interstitial fluid velocity and pore diffusivity of a solute as the pore connectivity, n_T, of the porous medium is varied from 2.6 to 6.0. The results show that the intraparticle interstitial velocity and the pore diffusivity increase significantly as the value of the pore connectivity, n_T, increases, and clearly indicate that the pore connectivity, n_T, plays a key role in determining the mass transport properties of a porous medium and, therefore, it is an extremely important parameter in the characterization and construction of porous particles. Furthermore, the results show that the intraparticle interstitial fluid velocity, $v_{p,i}$, is many times larger than the diffusion velocity, v_{DA}, of the solute within the porous medium, and the ratio $v_{p,i}/v_{DA}$ increases significantly as the pore connectivity, n_T, increases. The results of this work indicate that the pore network model could allow one, for a given porous medium, solute and interstitial column fluid velocity, to determine the values of the intraparticle interstitial fluid velocity, $v_{p,i}$, and pore diffusivity, D_p, of the solute in an a priori manner. The values of $v_{p,i}$ and D_p could then be employed in the macroscopic models that describe the dynamic behavior of chromatographic separations in columns packed with porous particles.

Keywords: Network model; Pore size distribution; Pore connectivity; Intraparticle convection; Intraparticle diffusion; Porous particles; Perfusion chromatography; Percolation threshold

1. Introduction

Protein purification with high separation speed could be obtained in columns packed with chromatographic porous particles whose porous structure allows the transport of the molecules of interest to occur by intraparticle convective fluid flow and pore diffusion [1–21]. Furthermore, Liapis [12] has shown that significant increases in the throughput, for a given pressure drop over the total length of the chromatographic column could be obtained if the packed bed of the column, is made with porous chromatographic particles that allow intraparticle fluid flow and have a partially fractal structure. The theoretical models [5–20] developed to describe the dynamic behavior of columns packed with porous chromatographic particles allowing intraparticle convection and diffusion have involved macroscopic modeling of the chromatographic particles and column properties and have analyzed and emphasized the enhancement of column efficiency, due to intraparticle fluid flow, at high flow-rates. The macroscopic models lump the pore structure characteristics of the pore size distribution (PSD) and pore connectivity, n_T, into the empirical tortuosity factor, τ, in the constitutive equations describing mass transfer in the porous chromatographic particles. Therefore, one does not have an understanding of the relationship

*Corresponding author.

0021-9673/98/$ – see front matter
PII: S0021-9673(98)00658-X

between the pore structure characteristics (PSD and n_T) and intraparticle fluid flow and pore diffusion in the porous particles; for this reason, one cannot estimate in an a priori manner the values of the effective pore diffusivity and intraparticle fluid flow in the porous chromatographic particles. While the macroscopic models have successfully described the dynamic behavior of column systems, the values of their parameters that characterize pore diffusion and intraparticle fluid flow have been determined in an a posteriori manner by matching dynamic experimental data with the predictions of the macroscopic models; furthermore, no relationship has been established through the use of macroscopic models between the pore structure characteristics and the values of the effective pore diffusion coefficient and intraparticle fluid flow.

Discrete pore network models, which incorporate the pore size distribution of the pore space and the pore connectivity between the pores of the porous medium, have been constructed [22–34] in order to provide a more realistic representation of the pore space in porous media. In pore network models, the porous structure is represented by a two-dimensional or a three-dimensional network (lattice) of nodes that are interconnected by bonds representing the pores. The pore network is constructed using a Monte Carlo simulation procedure where cylindrical pores are randomly assigned to the bonds of the network and the diameters of the assigned pores are distributed according to a pore size distribution, which is inferred [30,34–36] by simulating mercury intrusion on the network models and comparing the simulations with experimental mercury intrusion data. Discrete pore network models could allow one to (i) study directly the transport phenomena within the pore space of the porous media [25,27,28,31,32,37,38], (ii) correlate directly the effects of pore size distribution and pore connectivity with the parameters that characterize the mechanisms of pore diffusion and intraparticle fluid flow in the porous particles and (iii) estimate the values of the effective pore diffusion coefficient and the intraparticle fluid flow in the porous medium in an a priori manner. Petropoulos et al. [27,31] and Petrou et al. [28] developed two-dimensional pore network models and constructed the expressions and the approach for evaluating the pore diffusion and surface diffusion coefficients of adsorbate molecules in monodisperse and bidisperse porous adsorbent particles. They determined quantitatively the effects of the pore size distribution and pore connectivity of the porous adsorbent particles, as well as the effects of the size of the adsorbate molecule, the size of the immobilized active site, and the degree of saturation of the active sites on the effective pore diffusion coefficient of the adsorbate in the porous particles. Furthermore, they demonstrated certain important characteristic effects of non-random bidisperse pore structure on transport behavior and their practical consequences, especially in connection with the experimental determination of surface diffusion coefficients [31]. Liapis et al. [37] recently studied the frontal chromatography of proteins in columns packed with porous adsorbent particles whereby the effective pore diffusion coefficient of the adsorbate molecules in the porous particles was being determined as pore diffusion and adsorption were occurring in the particle, through the use of a pore network model. Loh and Wang [34] represented the packed column by a cubic lattice network of interconnected cylindrical pores and used their pore network model to simulate mercury intrusion, adsorption capacity and size exclusion chromatography. They arbitrarily considered [34] that there was no intraparticle fluid flow in pores whose diameter was in the pore diameter range 20–1000 Å (these pores were considered to represent only diffusive micropores) while the pores whose diameter was in the pore diameter range 1000 Å to about 1 μm were arbitrarily considered to represent the convective macropores where intraparticle fluid flow occurred. By studying in detail the text and the computer programs in Loh's doctoral dissertation [38], it was found [39] that the periodic boundary conditions of the cubic lattice were incomplete and, thus, the majority of the connections between corresponding edges of the cubic lattice were missing. This resulted in a smaller connectivity across the periodic planes than that reported [34,38]. Furthermore, Loh's pore size distribution [34,38] had significantly more interstitial pores, which would make his column porosity substantially higher than the values of 0.25 and 0.23 reported in his doctoral dissertation [38].

In this work, a cubic lattice network of interconnected cylindrical pores is constructed to repre-

sent a section of the packed column and is used to determine the intraparticle velocity for different values of the pore connectivity, n_T, of the porous particles and of the superficial velocity, $V_{b,sup}$, of the fluid in the column. Also, the network model that represents the pore structure characteristics of the porous particles is used to determine the values of the pore diffusion coefficient of two different solutes as the pore connectivity of the network model is varied.

2. System formulation

The packed column is topologically mapped onto a cubic lattice network of interconnected cylindrical pores and the lattice employed in our work has a regular array of nodes (the lattice size, L, is the same along the x, y and z space coordinates of the network and, thus, $x \times y \times z$:$L \times L \times L$) that are connected to each other by bonds (pores) of the network. The porous structure in the packed column has (a) interstitial pores which represent the pores between the packed-in-the-column particles and provide the flow channels for bulk fluid flow in the column and (b) intraparticle pores which represent the pores within the porous particles. The intraparticle pores may have (i) a monodisperse pore size distribution or (ii) a bidisperse pore size distribution. In case (ii), the pores inside the particle may be subdivided into macropores and micropores. The nodes of the cubic lattice are considered to have no volume in the network while the bonds (pores) of the network are considered to provide the pore volume of the network. In Fig. 1, a schematic representation of a column section packed with porous particles is shown, and the composite pore size distribution representing the porous structure of a small finite section of the column packed with porous particles having macropores and micropores (the pore size distribution of the pores of the particles is considered to be bimodal) is constructed topologically in the lattice by randomly assigning cylindrical pores to the bonds in the cubic network. It should be noted that the schematic representation of the model porous medium in Fig. 1 reflects an 'actual' model porous medium structure taking into account pore length variability. For the realistic representation of the

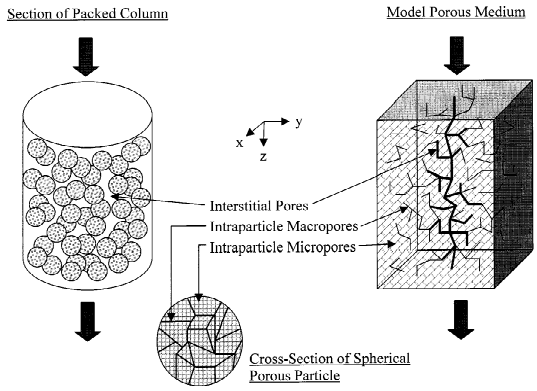

Fig. 1. Schematic representation through the pore network model of a finite small section of a packed bed.

porous structure in the column, the pore size distribution of the network (model porous medium) should be similar to the pore size distributions encountered in the interstitial pores and in the pores of the particles. In a column being in operation in practice, the interstitial and intraparticle pores are correlated [32] and, thus, cannot be assigned to the network randomly. Therefore, in order to generate a realistic model porous medium (network) representation of the packed column, the interstitial pores are assigned [34,39] in a semi-random manner to a percolating cluster that transects the lattice. The assignment of the intraparticle pores in the network is completely random. It should be noted here that there could exist certain porous chromatographic particles in which the macropores are not randomly distributed relative to the micropores (non-random bidisperse pore network); in such a case, our approach in constructing the intraparticle pore network would have to be slightly modified by employing in the assignment of the intraparticle pores the procedure developed by Petrou et al. [28] and Petropoulos et al. [31]. In this work, results are also presented for a porous medium where certain intraparticle macropores are not randomly distributed in the intraparticle pore network. For all of the simulations presented in this work, a lattice size of $15 \times 15 \times 15$ was used, which, from previous experience with random networks [28,31], would be expected to provide a reasonably satisfactory representation of the pore network and does not require excessive computational times. The details of the

construction of the lattice network and the computational methods employed in this work are presented in the report of Meyers [39].

The functional form of the composite pore size distribution representing the porous structure and the value of the pore connectivity for the interstitial and intraparticle pores could be determined from (i) digital image analyses on scanning electron microscopy (SEM) images, (ii) transmission electron microscopy (TEM), (iii) mercury intrusion simulation and comparison of the results with experimental mercury intrusion data, (iv) size-exclusion chromatography (SEC) and (v) studies involving adsorption capacity simulation and comparison of the results with experimental data. In this work, the following pore size distribution

$$f(d) = \sum_{i=1}^{3} \frac{\gamma_i}{\sqrt{2\pi}\sigma_i} \exp\left(-\frac{1}{2}\left(\frac{d-\mu_i}{\sigma_i}\right)^2 \right) \quad (1)$$

has been employed in the simulations. This pore size distribution is made up of the sum of three Gaussian distributions in order to represent the interstitial pores ($i=1$) in the column, the intraparticle macropores ($i=2$) and the intraparticle micropores ($i=3$). The values of γ_1, γ_2 and γ_3 in Eq. (1) are 0.013, 2.48 and 2.0, and represent the relative proportions of the interstitial pores, macropores and micropores, respectively, in the packed column. The parameter, d, represents the pore diameter, μ_i ($i=1, 2, 3$) denotes the mean diameter of pores of class i, and σ_i (i=1, 2, 3) is the standard deviation of the diameter of pores of class i. The values of μ_i and σ_i in Eq. (1) are as follows: $\mu_1=4.40$ μm, $\mu_2=0.534$ μm, $\mu_3=0.039$ μm, $\sigma_1=1.30$ μm, $\sigma_2=0.38$ μm and $\sigma_3=0.030$ μm. The values of the total porosity, ε_t, of the column, the void fraction, ε, of the bed, and the particle porosity, ε_p, are 0.68, 0.36 and 0.50, respectively. The diameter of the particles considered in this work is 15 μm and the ratio of μ_1 (mean pore size of interstitial pores) to particle diameter is $(4.40/15)=0.293$. Different investigators have found [40,41], using various sphere packing models and mercury intrusion measurements, that the ratio of the mean diameter of the pores formed between the packed particles to the diameter of the particles is between 0.27 and 0.37, depending on the porosity of the packing. The ratio of $(4.40/15)=0.293$ utilized in this work is within the range of values reported in the literature. Our pore network model formulation can use any physically and mathematically appropriate functional form for the pore size distribution $f(d)$. Loh and Wang [34] found that the functional form for the pore size distribution, $f(d)$, given by Eq. (1) could fit their pore size distribution data for the chromatographic particles examined in their work.

In the following paragraphs of this section, the quantitative expressions and methods for determining the intraparticle velocity and the pore diffusion coefficient of a solute in the porous particles, through the use of the pore network model constructed in this work, are presented.

2.1. Determination of the intraparticle fluid velocity

The pressure drop across a short cylindrical pore can be accurately determined to less than 1% in error by Eq. (2), which was constructed by Dagan et al. [42] for the pressure drop, Δp, through a cylindrical pore of finite length, l_p, under creeping flow conditions.

$$\Delta p = \left(\frac{16 l_p}{\pi d} + 3\right)\frac{8Q\mu}{d^3} \quad (2)$$

A pore in the pore network model is connected through nodes i and j and, thus, the flow-rate Q_{ij} through each pore in the network model can be obtained from Eq. (3) as follows:

$$Q_{ij} = \frac{(p_i - p_j)d^3}{\left(\left(\frac{128 l_p}{\pi d} + 24\right)\mu\right)} \quad (3)$$

The bond (pore) length, l_p, used in the construction of the lattice network can be related to the pore diameter, d, and can either be randomly assigned or constant. Dullien [43] reports that various photomicrographic investigations indicate that the length, l_p, of a pore is of the same order of magnitude as its diameter, d. In this work, the pore length, l_p, is taken to be equal to the diameter of the pore, d, since network simulations of porous media [29,44] have shown that network model predictions for mass transfer parameters based on all of the various methods used to assign pore lengths, agree well with

experimental data. In our pore network model, the pore length, l_p, could be assigned in any of the above-mentioned methods, and the assignment of l_p, to be equal to d in this work, is considered to be topologically reasonable in light of the findings of the above-mentioned researchers [29,43,44]. By letting $l_p = d$ in Eq. (3) the following expression for the evaluation of the flow rate Q_{ij}, is obtained:

$$Q_{ij} = \frac{(p_i - p_j)d^3}{\left(\left(\frac{128}{\pi} + 24\right)\mu\right)} \tag{4}$$

The nodal pressures are obtained from the solution of a set of linear equations that are constructed by rewriting Eq. (4) in terms of the net mass flow at node i [39]. Since all of the flow on the top surface (first layer of nodes that is perpendicular to the direction of mass transfer) goes through the first layer of pores of the network, the nodes on the top surface can be reduced to one node whose net mass flow at the node is equal to the total mass flow. The situation is similar for the bottom surface, since all of the flow comes out of the network onto the bottom surface, and this surface can be reduced to one node whose net mass flow is the negative of the total. Lastly, for every interior node, since mass is conserved, the net mass flow is equal to zero. After the solution of the background pressures has been obtained, the pressure drop through the interstitial pore cluster of the network is determined and, thus, the amount of flow, Q_i, through the interstitial pores is calculated. Then the amount of intraparticle flow, Q_p, through the porous structure of the particles is obtained by subtracting the amount of flow through the interstitial pores from the total flow, Q_t, through the bed ($Q_p = Q_t - Q_i$). By letting $Q_t = V_{b,sup} S_c$ and $Q_p = v_{p,sup} S_c(1-\varepsilon)$ (where S_c is the cross-sectional area of the column, $V_{b,sup}$ denotes the superficial velocity of the fluid in the column, and $v_{p,sup}$ represents the superficial intraparticle velocity), the ratio of the superficial intraparticle fluid velocity to the superficial velocity of the fluid in the column is given by the following expression:

$$\frac{v_{p,sup}}{V_{b,sup}} = \left(\frac{1}{1-\varepsilon}\right)\left[\frac{Q_p}{Q_t}\right] \tag{5}$$

The ratio of the intraparticle interstitial velocity, $v_{p,i}$ ($v_{p,i} = v_{p,sup}/\varepsilon_p$), to the interstitial bed velocity, $V_{b,i}$ ($V_{b,i} = V_{b,sup}/\varepsilon$), could provide more useful practical information when one compares the relative speeds of movement of the solute inside the pores of the particle due to intraparticle fluid flow and pore diffusion. The ratio of $v_{p,i}$ to $V_{b,i}$ is as follows:

$$\frac{v_{p,i}}{V_{b,i}} = \left(\frac{\varepsilon}{\varepsilon_p}\right)\left[\frac{v_{p,sup}}{V_{b,sup}}\right] = \left(\frac{\varepsilon}{\varepsilon_p(1-\varepsilon)}\right)\left[\frac{Q_p}{Q_t}\right] \tag{6}$$

2.2. Determination of the intraparticle pore diffusivity

The diffusion rate of the molecules of species A having effective molecular radius α_1 through a single cylindrical pore of length l_p, and radius r_p ($r_p = d/2$) is given by the following expression [27] when a linear concentration gradient is considered to exist within the liquid in the pore and adsorption does not take place

$$J_{DA} = \pi r_p^2 K_A D_A \left(\frac{\Delta C_A}{l_p}\right) = P'_{DA}\left(\frac{\Delta C_A}{l_p}\right) = \pi r_p^2 P_{DA}\left(\frac{\Delta C_A}{l_p}\right) \tag{7}$$

where P'_{DA} denotes 'permeance' = permeability(P_{DA}) × cross-sectional area. For certain chromatographic systems, it is possible that, under certain conditions, the concentration gradient in the pore is nonlinear; in this case, one would have to integrate the material balance equation of the diffusing species for each pore. The total restriction to diffusion due to the combined effects of steric hindrance at the entrance to the pore and frictional resistance within the pore may be considered (to a first approximation) to be provided by the expression proposed by Renkin [45], and the term $K_A D_A$ is given by

$$K_A D_A = D_{mf}\left(1 - \frac{\alpha_1}{r_p}\right)^2\left[1 - 2.104\left(\frac{\alpha_1}{r_p}\right) + 2.09\left(\frac{\alpha_1}{r_p}\right)^3 - 0.95\left(\frac{\alpha_1}{r_p}\right)^5\right] = D_{mf}\varphi(r_p, \alpha_1) \tag{8}$$

where D_{mf} represents the free molecular diffusion coefficient of species A. Brenner and Gaydos [46] and Mason et al. [47] have also proposed other functional forms for $\varphi(r_p, \alpha_1)$, but numerous calcula-

tions indicate that there are small differences between the results obtained from Eq. (8) and the expressions suggested in references [46,47].

The basic expression for the mass flux, $N_{DA,ij}$, of the molecules of species A through a cylindrical pore of length, l_p, can be employed in order to determine the concentration difference through the pore connected to nodes i and j. The expression for $N_{DA,ij}$ is given by Eq. (9)

$$N_{DA,ij} = \frac{J_{DA,ij}}{\pi(r_{p,ij})^2} = (K_A D_A)_{ij}\left(\frac{C_i - C_j}{l_{p,ij}}\right) = D_{mf}\varphi(r_{p,ij}, \alpha_1)\left(\frac{C_i - C_j}{l_{p,ij}}\right) \quad (9)$$

However, for a three-dimensional network of cylindrical pores (as is the network used in this work), it is more convenient to write expressions for the net flux at each node in order to calculate the nodal concentrations. Since the mass flux given on the top surface (first layer of nodes which is perpendicular to the direction of the net mass transfer) of the network is the same as the sum of the mass fluxes of the pores emanating from this surface into the network, the top layer of nodes can be reduced to a single node (node 1). The net mass flux between this node and all of the nodes of the second layer is equal to the specified total mass flux, N_{DAo}, and is given by the following expression

$$\sum_{j=1}^{N_a} N_{DA,1j} = \sum_{j=1}^{N_a} (K_A D_A)_{1j}\left(\frac{C_1 - C_j}{l_{p,1j}}\right)\delta_j = N_{DAo} \quad (10)$$

where N_{DAo} is the flux specified (set) at node 1, N_a represents the total number of nodes in the cubic lattice network, and δ_j is equal to one when an adjacent node is connected by a pore (bond) to node 1 while δ_j is equal to zero when an adjacent node is not connected by a pore to node 1. Similarly, the bottom surface of the network can be reduced to a single node (node N_e) where the sum of the mass fluxes emanating from the last layer of nodes of the network to node N_e is equal to the negative of the total specified mass flux, N_{DAo}, and is given by the expression

$$\sum_{j=1}^{N_a} N_{DA,N_e j} = \sum_{j=1}^{N_a} (K_A D_A)_{N_e j}\left(\frac{C_{N_e} - C_j}{l_{p,N_e j}}\right)\delta_j = -N_{DAo} \quad (11)$$

where δ_j is equal to one when an adjacent node is connected by a bond (pore) to node N_e, while δ_i is equal to zero when an adjacent node is not connected by a pore to node N_e. Then, for every interior node (nodes on the second through the fifteenth layers, where a layer is the plane surface perpendicular to the net mass flux direction), the net mass flux must be equal to zero, as shown in Eq. (12)

$$\sum_{j=1}^{N_a} N_{DA,ij} = \sum_{j=1}^{N_a} (K_A D_A)_{ij}\left(\frac{C_i - C_j}{l_{p,ij}}\right)\delta_j = 0 \quad (12)$$

where δ_j is equal to one when node i is connected to adjacent node j by a pore (bond) while δ_j is equal to zero when node i is not connected by a pore to adjacent node j. The simultaneous solution of Eqs. (10)–(12) provides the value of the concentration of species A at each node of the network. In order to determine the pore diffusivity, D_p, of species A in the model porous medium, the total permeability, P, of species A in the model porous medium must first be calculated. The total permeability, P, is calculated from Eq. (13)

$$P = \left(\frac{1}{2}\right)\left(\frac{1}{S_0}\right)\left[\sum_{i=1}^{N_a}\sum_{j=1}^{N_a} P'_{DA,ij}\left(\frac{\Delta c_{ij}}{\nu_{ij}}\right)\right] \quad (13)$$

where N_a represents the total number of nodes in the network; $P'_{DA,ij} = \pi(r_{p,ij})^2(K_A D_A)_{ij} = \pi(d/2)^2_{ij} \times (K_A D_A)_{ij}$; ν_{ij} represents the ratio of the pore length $l_{p,ij}$ to the shortest distance connecting node i with another adjacent node; S_0 is the cross-sectional area of the model porous medium and Δc_{ij} represents the normalized concentration difference where

$$c_i = \frac{(C_i - C_{N_e})}{(C_1 - C_{N_e})}; \quad c_1 = 1; \quad c_{N_e} = 0 \quad (14)$$

The factor $1/2$ in Eq. (13) allows for counting each capillary twice in the summation. Also, although there are concentration gradients through pores on the plane (x, y) perpendicular to the direction (z) of net mass transfer, it is the pores in the z direction that contribute to the net flux. For this reason, Eqs. (10)–(12) are solved for all nodes in the network of intraparticle pores taking into account all intraparticle pores so as to determine a concentration gradient for each pore, while Eq. (13) is calculated for all nodes taking into account only the pores in the direction (z) of net mass transfer.

The pore diffusion coefficient, D_p, of the molecules of species A in the porous medium is then obtained from Eq. (15)

$$D_p = \frac{P}{\varepsilon_p} \tag{15}$$

where the value of P is determined from Eq. (13). It is worth noting again at this point that, in Eqs. (7)–(13), the value of r_p is equal to $d/2$ (d represents the pore diameter) and the pore length l_p is set equal to the pore diameter d in the construction of the pore network model, for the reasons discussed above.

3. Results and discussion

In Figs. 2–6, the results obtained from the pore network are presented for the case where the intraparticle macropores are randomly distributed relative to the micropores (Case I). Simulation of the model porous medium using the PSD mentioned above (Eq. (1)) yields a percolation threshold at pore connectivity of 2.6. Connectivities below this value do not produce a percolating cluster of interstitial pores, which is necessary for flow through the model porous bed. In Fig. 2, the ratio of the intraparticle interstitial velocity, $v_{p,i}$, to the interstitial column fluid velocity, $V_{b,i}$, versus the pore connectivity, n_T, is presented. The results in Fig. 2 indicate that the value of the ratio $v_{p,i}/V_{b,i}$ increases significantly as the pore connectivity, n_T, of the intraparticle pores increases. It can be observed that when n_T is equal to 2.6, the value of $v_{p,i}/V_{b,i}$ is about 3.04×10^{-3}, while when n_T is equal to six, which means that the lattice network is completely occupied, since, in this case, the value of n_T is equal to the coordination number of the cubic lattice, the value of $v_{p,i}/V_{b,i}$ has increased to about 1.85×10^{-1}. In Fig. 3, the ratio $v_{p,i}/V_{b,i}$ versus $V_{b,i}$ is plotted for different values of the pore connectivity, n_T. The results in Fig. 3 clearly show that for a given value of the pore connectivity, n_T, the ratio $v_{p,i}/V_{b,i}$ is constant and independent of the value of the interstitial column fluid velocity, $V_{b,i}$; this result is as it should be

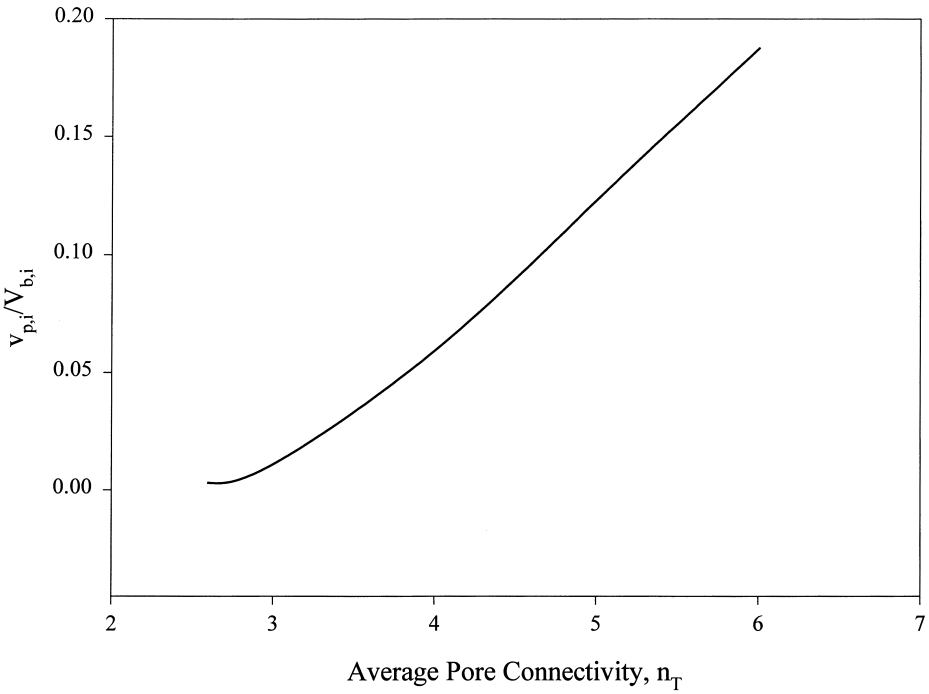

Fig. 2. Ratio of intraparticle interstitial velocity, $v_{p,i}$, to interstitial column fluid velocity, $V_{b,i}$, versus the average pore connectivity, n_T, of the porous medium for Case I.

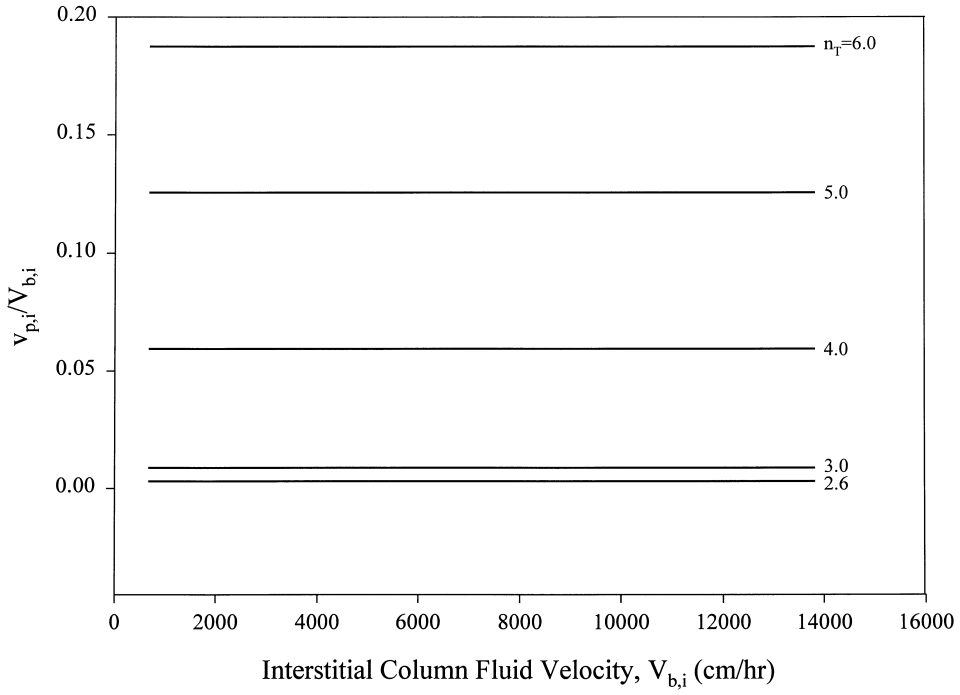

Fig. 3. Ratio of intraparticle interstitial velocity, $v_{p,i}$, to interstitial column fluid velocity, $V_{b,i}$, versus the interstitial column fluid velocity, $V_{b,i}$, for different values of the average pore connectivity, n_T, of the porous medium for Case I.

because the value of the ratio $v_{p,i}/V_{b,i}$ depends only on the microscopic characteristics of the intraparticle pore structure, which are determined from the pore size distribution and pore connectivity of the porous medium. The results in Figs. 2 and 3 indicate that the pore network model could allow one to determine, for a given porous medium of interest and for a given value of the interstitial column fluid velocity, $V_{b,i}$, the value of the intraparticle interstitial fluid velocity, $v_{p,i}$, in an a priori manner. This is a very significant result and can be used to provide in an a priori manner numerical values for the intraparticle velocity components v_{pR} and $v_{p\theta}$ (along the R and θ coordinate directions of the spherical porous particle), which are utilized in the macroscopic models [13–20] that describe the dynamic behavior of chromatographic separations in columns packed with porous particles. The intraparticle velocity components v_{pR} and $v_{p\theta}$ can be obtained from the expressions [14]

$$v_{pR} = F(\varepsilon V_{b,i}) \cos\theta \tag{16}$$

$$v_{p\theta} = -F(\varepsilon V_{b,i}) \sin\theta \tag{17}$$

where

$$F = \frac{v_{p,i}}{\varepsilon V_{b,i}} \tag{18}$$

By determining the value of $v_{p,i}$ from the pore network model in an a priori manner, as discussed above, the value of F is obtained from Eq. (18) and then the values of v_{pR} and $v_{p\theta}$ can be estimated from Eqs. (16) and (17), respectively.

In Fig. 4, the ratio of the pore diffusion coefficient, D_p, to the product of ε_p with D_{mf} versus the pore connectivity, n_T, is presented, for lysozyme and β-galactosidase. The values of α_1 and D_{mf} in Eq. (8) are as follows: for lysozyme, $\alpha_1 = 21.4$ Å and $D_{mf} = 1.006 \times 10^{-10}$ m^2/s; for β-galactosidase, $\alpha_1 = 70.6$ Å and $D_{mf} = 3.90 \times 10^{-11}$ m^2/s. The results in Fig. 4 clearly indicate that as the pore connectivity, n_T, increases, the value of the ratio $D_p/\varepsilon_p D_{mf}$ increases significantly. Lysozyme has a substantially higher ratio of $D_p/\varepsilon_p D_{mf}$ than β-galactosidase because the

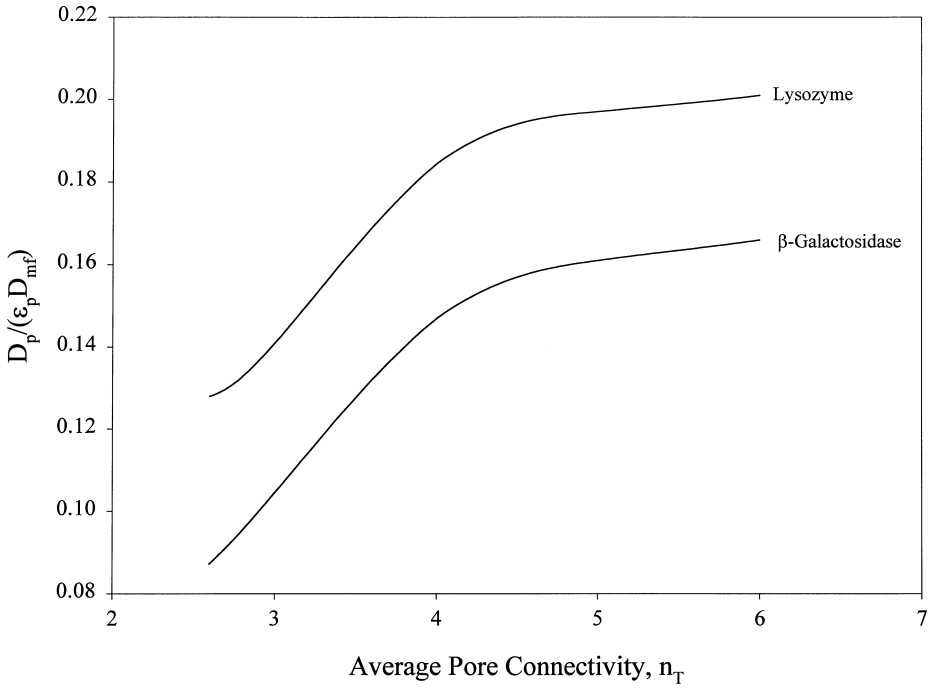

Fig. 4. Ratio of the effective pore diffusion coefficient, D_p, to $\varepsilon_p D_{mf}$ versus the average pore connectivity, n_T, of the porous medium for Case I.

size of the lysozyme molecule is smaller and, thus, it has a lower total restriction to diffusion due to the combined effects of steric hindrance at the entrance to each pore in the pore network and frictional resistance within each pore and, furthermore, the lysozyme molecule has access to more pores of the pore network than β-galactosidase. It can also be observed that the increase in the value of the ratio $D_p/\varepsilon_p D_{mf}$ with n_T in the range of values of n_T between 4.5 and 6 is significantly smaller than the increase in the value of $D_p/\varepsilon_p D_{mf}$ with n_T in the range of values of n_T between 2.6 and 4.5. This result is due to the fact that the pores in the pore network are significantly more interconnected when n_T is in the range 4.5–6. The data in Fig. 4 indicate that the pore network model could allow one to determine, for a given porous medium and for a given solute of interest, the pore diffusion coefficient, D_p, of the solute in an a priori manner. One does not need to estimate values for the empirical parameter of tortuosity since tortuous pathways for mass transfer are already built within the pore network model. Furthermore, the pore network model properly accounts for the overall restriction to diffusion (overall hindrance) due to steric hindrance at the entrance to the pores and frictional resistance within the pores, since each pore in the pore network employs the expression for $K_A D_A$ given in Eq. (8). If one would consider the empirical relationship $D_p = (\varepsilon_p D_{mf})(\lambda/\tau)$, where λ represents the hindrance parameter of the porous medium and τ denotes the average tortuosity in the porous medium, then the ratio $D_p/\varepsilon_p D_{mf}$ in Fig. 4 might be thought of as providing the value of the ratio λ/τ in an a priori manner. The results in Fig. 4 indicate that the pore network model can be used to provide in an a priori manner numerical values for the pore diffusion coefficient, D_p, which is employed in the macroscopic models [13–20] that describe the dynamic behavior of chromatographic separations in columns packed with porous particles.

In Figs. 5 and 6, the ratio of the intraparticle interstitial velocity, $v_{p,i}$, to the diffusion velocity, v_{DA}, versus the pore connectivity, n_T, is presented for lysozyme and β-galactosidase, respectively, and for different values of the interstitial column fluid

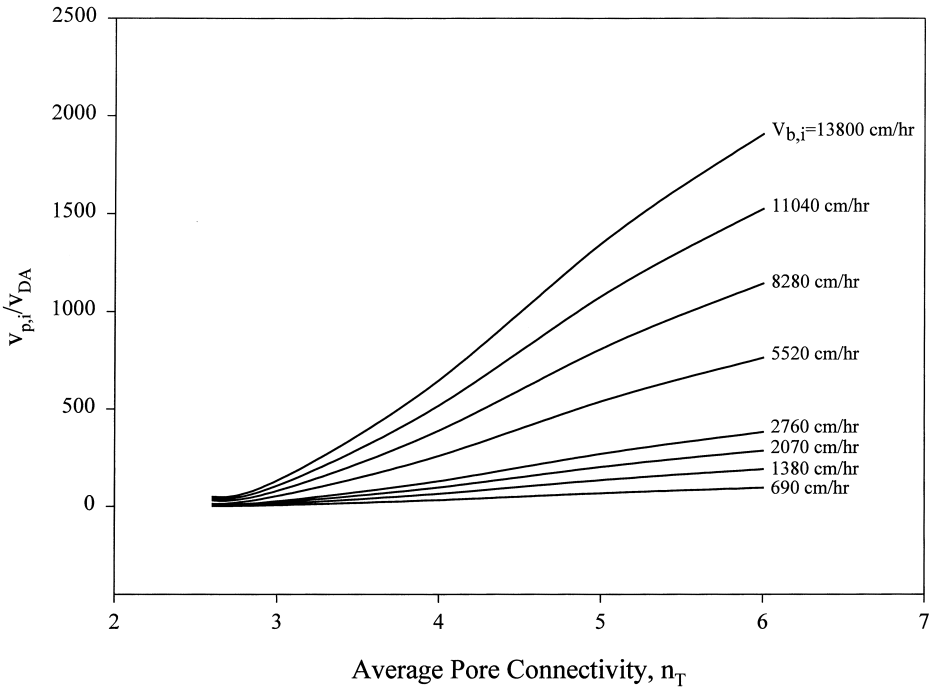

Fig. 5. Ratio of intraparticle interstitial velocity, $v_{p,i}$, to diffusion velocity, v_{DA}, of lysozyme versus the average pore connectivity, n_T, for different values of the interstitial column fluid velocity, $V_{b,i}$, for the porous medium of Case I.

velocity, $V_{b,i}$. The diffusion velocity, v_{DA}, could be estimated (Carlson and Dranoff [48]) from the ratio D_p/R_p where D_p is the pore diffusion coefficient of solute A and R_p represents the radius of the porous chromatographic particle; the value of R_p is 7.5 μm for the porous particles used here. It can be observed that the ratio $v_{p,i}/v_{DA}$ significantly increases as the pore connectivity, n_T, increases. It can also be observed that even at low values of n_T and $V_{b,i}$, the value of the intraparticle interstitial velocity, $v_{p,i}$, is orders of magnitude larger than the diffusion velocity, v_{DA}, and this indicates that the intraparticle interstitial velocity can significantly enhance the speed of the movement of the molecules of species A (lysozyme or β-galactosidase) inside the porous structure of the particles. The value of the ratio $v_{p,i}/v_{DA}$, for given values of n_T and $V_{b,i}$, is significantly larger for β-galactosidase because the diffusion velocity of β-galactosidase is substantially smaller than the diffusion velocity of lysozyme (compare the values of D_p for lysozyme and β-galactosidase in Fig. 4 and consider that each solute travels by diffusion a distance equal to the radius of the porous particle).

In Figs. 7–11, the results obtained from the pore network model are presented for the case where all of the intraparticle macropores with pore diameters greater than 1 μm are not randomly distributed relative to the other intraparticle pores, and are added through a random network connected with a high frequency to the pore cluster of the interstitial pores (Case II); this case would represent porous particles having on their outer surface a higher incidence of macropores that could permeate into the interior of the porous particles. The results in Fig. 7 indicate that the ratio $v_{p,i}/V_{b,i}$ increases substantially as the pore connectivity, n_T, increases. It can be observed that when n_T is equal to 2.6, the value of $v_{p,i}/V_{b,i}$ is 5.05×10^{-2}, while when n_T is equal to 6, the value of $v_{p,i}/V_{b,i}$ has increased to 2.83×10^{-1}. By comparing the results in Figs. 2 and 7, it is observed that, for the porous medium where the macropores are randomly distributed relative to the micropores (Fig. 2), the value of $v_{p,i}/V_{b,i}$ is about an order of

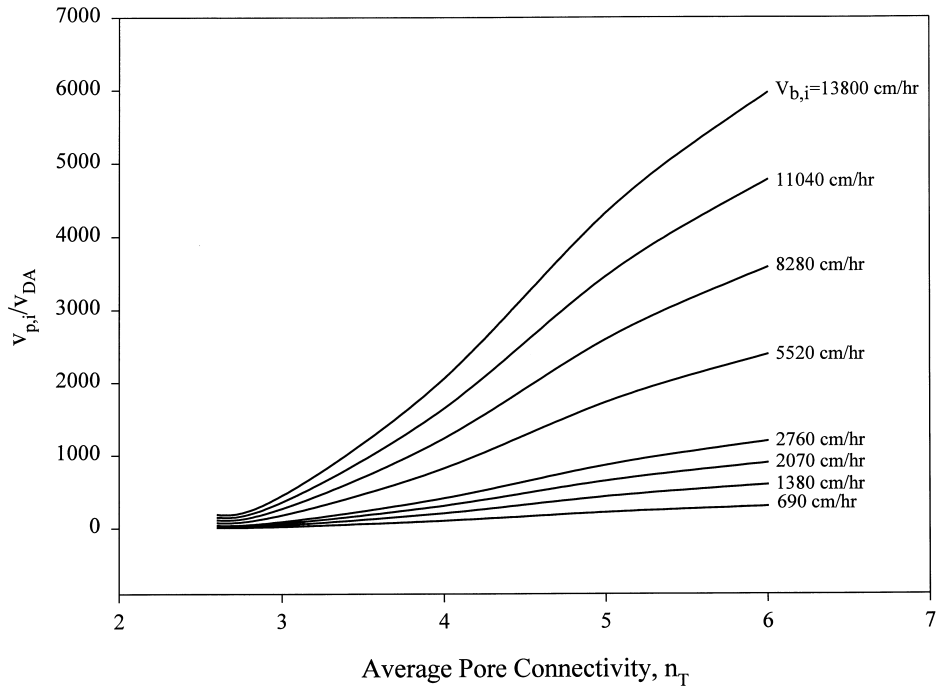

Fig. 6. Ratio of intraparticle interstitial velocity, $v_{p,i}$, to diffusion velocity, v_{DA}, of β-galactosidase versus the average pore connectivity, n_T, for different values of the interstitial column fluid velocity, $V_{b,i}$, for the porous medium of Case I.

magnitude lower when low values of n_T are considered, than the value of $v_{p,i}/V_{b,i}$ obtained for the porous medium presented in Fig. 7. As the value of n_T increases above about 4.5, the value of $v_{p,i}/V_{b,i}$ in Fig. 7 is still higher than the value of $v_{p,i}/V_{b,i}$ in Fig. 2, but it is now higher by a factor of about 1.6 and not by an order of magnitude; this decrease in the difference of the values of $v_{p,i}/V_{b,i}$ as n_T increases above about 4.5 is due to the fact that, at higher pore connectivities, the pores in the porous network are significantly more interconnected and, thus, a substantial relative increase in mass transfer occurs in the porous medium where the macropores are randomly distributed relative to the micropores (Fig. 2). The relative increase in mass transfer as n_T increases above 4.5 in the porous medium represented in Fig. 7 is not as large as the relative increase in mass transfer occurring in the porous medium of Fig. 2 because the effect on mass transfer of a value of n_T above 4.5 is more significant for Case I than for Case II. The results in Fig. 8 clearly show, as was the case in Fig. 3, that, for a given value of the pore connectivity, n_T, the ratio $v_{p,i}/V_{b,i}$ is constant and independent of the value of the interstitial column fluid velocity, $V_{b,i}$, indicating clearly that the value of the ratio $v_{p,i}/V_{b,i}$ depends only on the microscopic characteristics of the intraparticle pore structure, which are determined from the pore size distribution and pore connectivity of the porous medium.

Gustavsson et al. [21] have recently made direct measurements of the intraparticle interstitial velocity in the pores of superporous agarose beads and report that the intraparticle interstitial fluid velocity was determined to be 2–24% of the interstitial column fluid velocity for the different particle sizes of superporous agarose beads studied in their work. The pore size distribution (Eq. (1)) of the 15 μm particle diameter porous beads, studied through the network model developed in this work, indicates that there are many large diameter intraparticle pores in the particle that allow the intraparticle interstitial velocity to become (as % of the interstitial column fluid velocity) significant as the value of the pore connectivity, n_T, of the intraparticle pores increases (see the

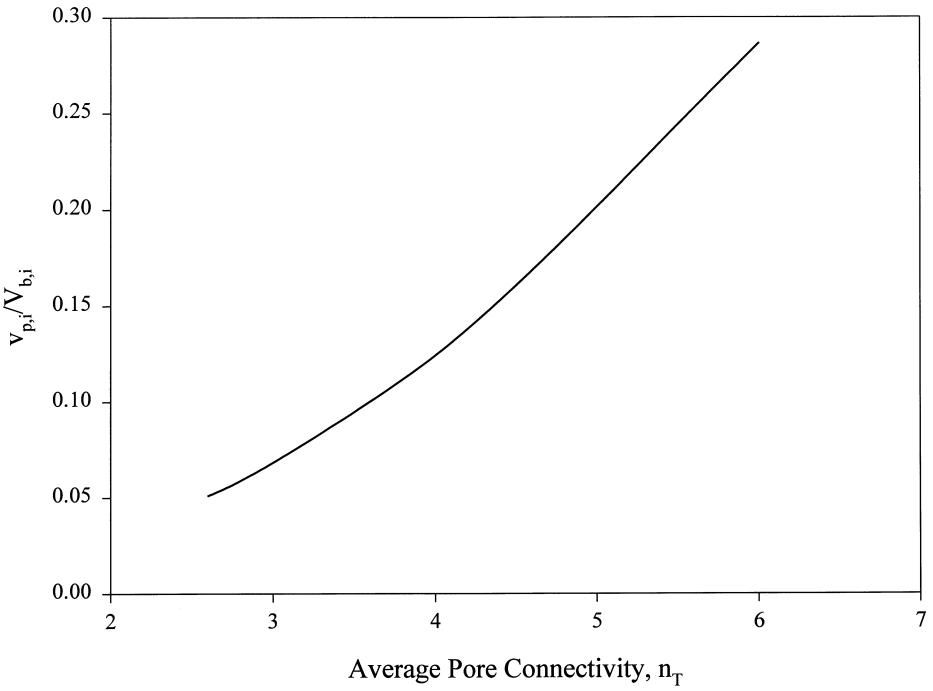

Fig. 7. Ratio of intraparticle interstitial velocity, $v_{p,i}$, to interstitial column fluid velocity, $V_{b,i}$, versus the average pore connectivity, n_T, of the porous medium for Case II.

results in Figs. 2, 3, 7 and 8). The main differences between the system of Gustavsson et al. [21] and the one considered in our work are that both (i) the size of the species transported in the pores of the particles used by Gustavsson et al. [21] and (ii) the size of the pores in their porous particles are larger than those considered in our work, but the physical trends with respect to intraparticle convective mass transfer are similar in both systems.

In Fig. 9, as was the case with the data in Fig. 4, the results show that the pore diffusivity significantly increases as n_T increases, and the pore diffusivity of lysozyme is substantially higher than that of β-galactosidase for the reasons presented above, where the results of Fig. 4 were discussed. The results in Fig. 9 also indicate that the value of the ratio $D_p/\varepsilon_p D_{mf}$ for lysozyme does not significantly increase with the pore connectivity, n_T, as the value of n_T increases above about 4.5. This implies that, at a pore connectivity of about 4.5 and higher, the pore network is so highly connected for the diffusion of the lysozyme molecules that an increase of the value of n_T above 4.5 insignificantly affects the value of D_p for lysozyme. This is not the case for β-galactosidase, and one can observe that, for this solute, the value of $D_p/\varepsilon_p D_{mf}$ continuously increases as n_T increases. By comparing the results in Figs. 4 and 9, it is observed that the pore network model of the system represented in Fig. 9 has higher pore diffusivities for lysozyme and β-galactosidase than the pore network model of the system represented in Fig. 4. Furthermore, it can be observed that the pore diffusivity of lysozyme obtained from the pore network model of the system represented in Fig. 9, does not change significantly when the pore connectivity, n_T, is about 4.5 and higher; this is not the case for the pore diffusivity of lysozyme determined from the pore network model of the system represented in Fig. 4.

In Figs. 10 and 11, the ratio of $v_{p,i}/v_{DA}$ versus n_T is presented for lysozyme and β-galactosidase, respectively, and for different values of the interstitial column fluid velocity, $V_{b,i}$. The effect of increasing the value of n_T on $v_{p,i}/v_{DA}$ is similar to that observed in Figs. 5 and 6. However, by comparing the results in Figs. 5 and 10 and in Figs. 6 and 11, it

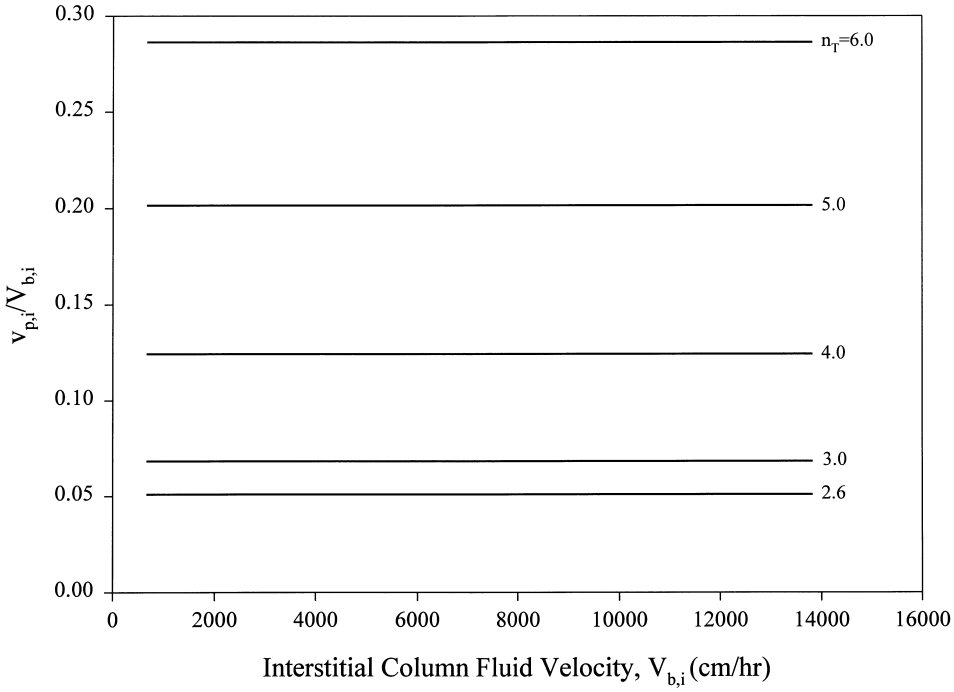

Fig. 8. Ratio of intraparticle interstitial velocity, $v_{p,i}$, to interstitial column fluid velocity, $V_{b,i}$, versus the interstitial column fluid velocity, $V_{b,i}$, for different values of the average pore connectivity, n_T, of the porous medium for Case II.

is observed that, at low values of n_T, the value of $v_{p,i}/v_{DA}$ in the pore network model of the system represented in Figs. 5 and 6 does not increase with increasing values of $V_{b,i}$ as much as the values of $v_{p,i}/v_{DA}$ in the pore network model of the system represented in Figs. 10 and 11. Also, Figs. 10 and 11 provide, for a given value of n_T, higher values of $v_{p,i}$ and D_p than those obtained in the pore network model of the system represented in Figs. 5 and 6.

4. Conclusions and remarks

A cubic lattice network of interconnected cylindrical pores was constructed to represent the porous structure existing in a column packed with porous chromatographic particles having intraparticle macropores and micropores. The microscopic properties of the porous network model are characterized by the pore size distribution and the pore connectivity, n_T, of the porous medium. Two different cases were examined with respect to the assignment of the intraparticle pores in the network model. In one case (Case I), the assignment of the intraparticle pores (macropores and micropores) is completely random and, thus, the macropores are randomly distributed relative to the micropores. In the second case (Case II), all of the intraparticle macropores with pore diameters greater than 1 μm are not randomly distributed relative to the other intraparticle pores, and are added through a random network connected with a high frequency to the pore cluster of the interstitial pores; this case would represent porous particles having on their outer surface a higher incidence of macropores that could permeate into the interior of the porous particles. In both cases, the interstitial pores are assigned in a semi-random manner to a percolating cluster that transects the lattice.

Expressions were constructed and used to determine, through the use of the pore network model, the intraparticle interstitial velocity and pore diffusivity of a solute as the pore connectivity, n_T, of the porous medium was varied from 2.6 to 6.0. Two

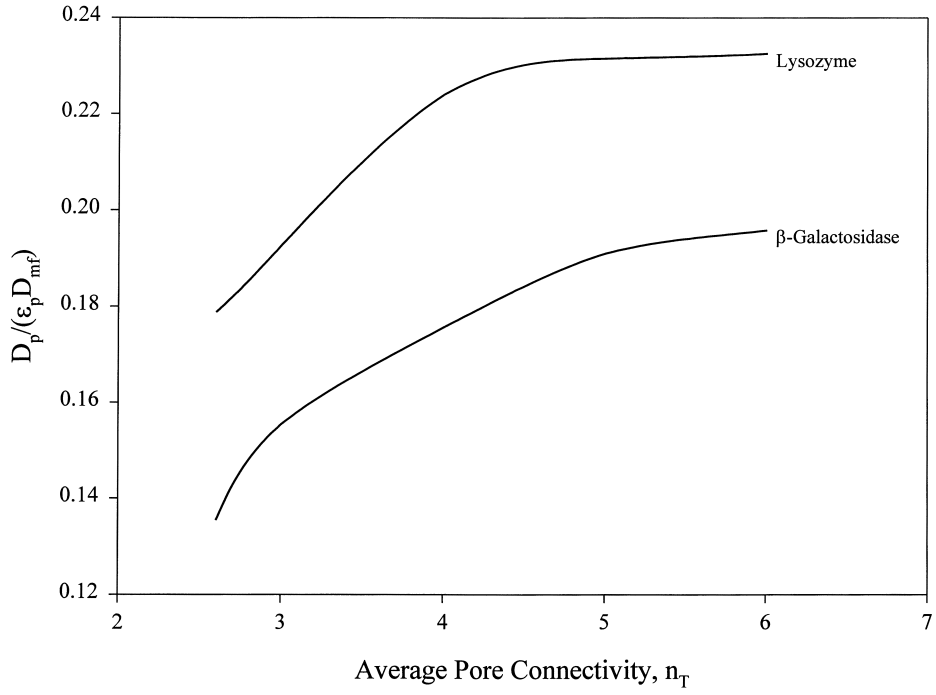

Fig. 9. Ratio of the effective pore diffusion coefficient, D_p, to $\varepsilon_p D_{mf}$ versus the average pore connectivity, n_T, of the porous medium for Case II.

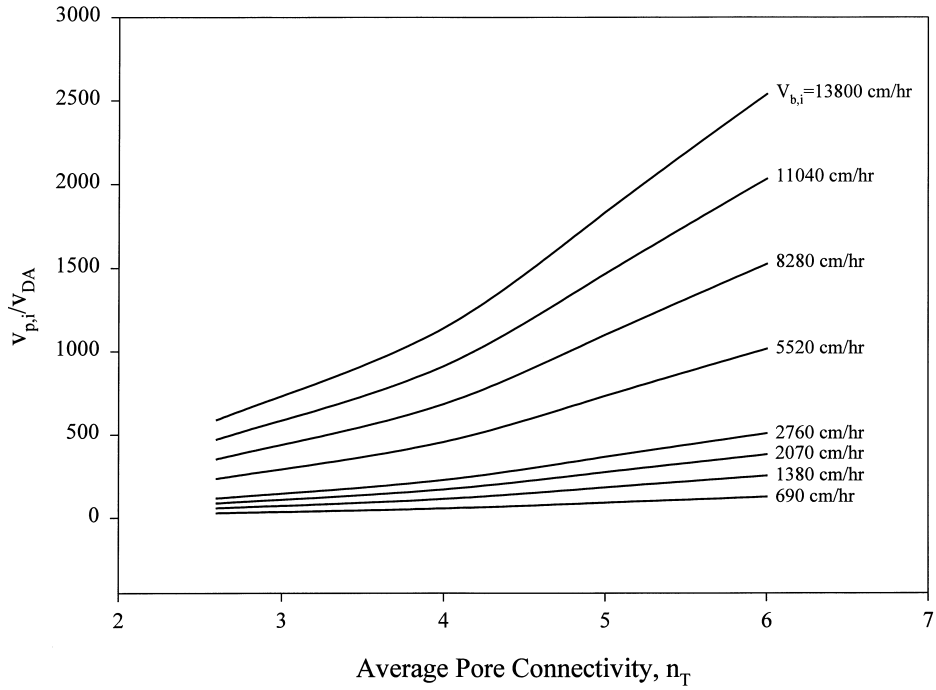

Fig. 10. Ratio of intraparticle interstitial velocity, $v_{p,i}$, to diffusion velocity, v_{DA}, of lysozyme versus the average pore connectivity, n_T, for different values of the interstitial column fluid velocity, $V_{b,i}$, for the porous medium of Case II.

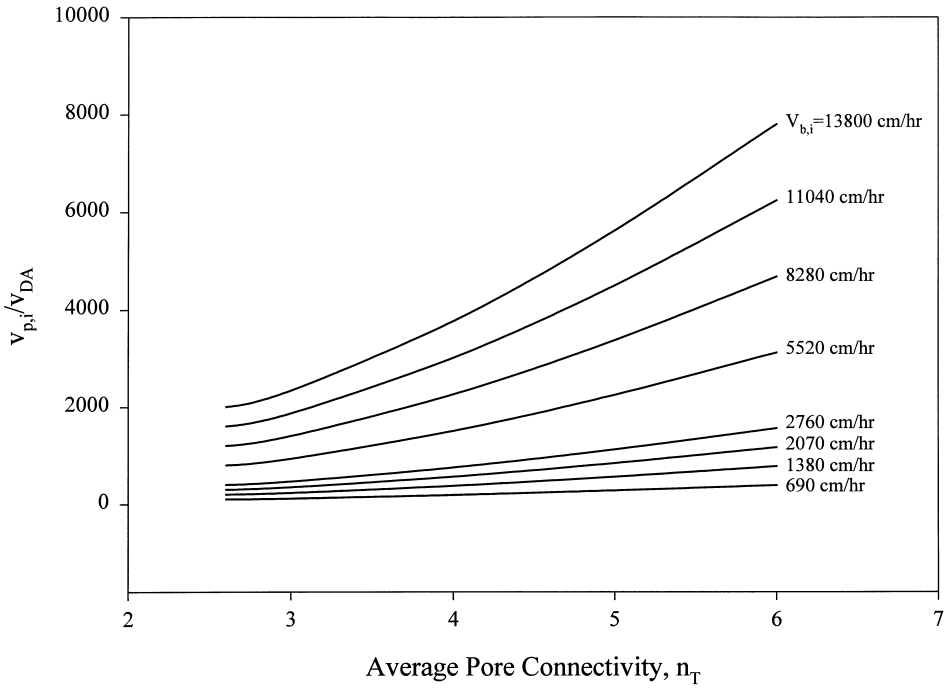

Fig. 11. Ratio of intraparticle interstitial velocity, $v_{p,i}$ to diffusion velocity, v_{DA}, of β-galactosidase versus the average pore connectivity, n_T, for different values of the interstitial column fluid velocity, $V_{b,i}$, for the porous medium of Case II.

different solutes were studied: lysozyme and β-galactosidase. The results show that the intraparticle interstitial velocity and the pore diffusivity increase significantly as the value of the pore connectivity, n_T, increases. They also clearly indicate that the pore connectivity plays a key role in determining the mass transport properties of a porous medium and, therefore, it is an extremely important parameter in the characterization and construction of porous particles. The results also indicate that the intraparticle porous structure of the network constructed for Case II is such that substantially higher intraparticle interstitial velocities and pore diffusivities are obtained, especially at lower values of the pore connectivity, n_T, than those obtained from the pore network model constructed for Case I. Also, the results of this work show that the magnitude of the intraparticle interstitial fluid velocity, $v_{p,i}$ is many times larger (orders of magnitude larger) than the diffusion velocity, v_{DA}, of the solute within the porous particle, and the ratio $v_{p,i}/v_{DA}$ increases significantly as the pore connectivity increases. This result clearly indicates that a certain amount of intraparticle fluid flow would be desirable because it would bring the adsorbate faster to the active sites immobilized on the surface of the pores. Of course, one would have to construct the adsorbent particle in such a way that (a) the intraparticle pores that allow flow are properly located in the topology of the porous medium, (b) their size and number are such that there is no large loss of internal surface area and (c) the chemistry of the active sites immobilized on the surface of the pores is such that the time constant of the interaction step between the active sites and the molecules of the adsorbate is significantly smaller than the time that it would take an adsorbate molecule to go through the particle by intraparticle fluid flow.

The results of this work indicate that the pore network model could allow one to determine for (i) a given porous medium of interest, (ii) a given solute of interest and (iii) a given value of the interstitial column fluid velocity, $V_{b,i}$, the values of the intraparticle interstitial fluid velocity, $v_{p,i}$, and pore diffusivity, D_p, of the solute in an a priori manner. This is a very significant result because the numerical values of $v_{p,i}$ and D_p determined in an a priori

manner through the use of the pore network model can be employed in the macroscopic models [13–20] that describe the dynamic behavior of chromatographic separations in columns packed with porous particles.

5. Notation

C_i, C_j concentration of solute A at nodes i and j, respectively, kg/m^3
D_A effective pore diffusion coefficient of solute A in a pore, m^2/s
D_{mf} free molecular diffusion coefficient of solute A, m^2/s
D_p effective pore diffusion coefficient of solute A in a porous medium (porous particle), m^2/s
d pore diameter, m
$f(d)$ functional form of pore size distribution
J_{DA} diffusion rate of solute A in a pore, kg/s
K_A effective distribution coefficient of solute A with respect to external solution
l_p pore length, m
N_{DA} mass flux of solute A in a pore due to diffusion, kg/(m^2·s)
n_T pore connectivity of the porous network (average number of pores connected at a node of the porous network)
P permeability of solute A in a porous medium (porous particle), m^2/s
P_{DA} permeability of solute A in a pore, m^2/s
P'_{DA} permeance of solute A in a pore, m^4/s
p_i, p_j pressure at nodes i and j, respectively, N/m^2
Q flow-rate through a pore, m^3/s
Q_i flow-rate through the interstitial pores in the column, m^3/s
Q_p intraparticle flow-rate, m^3/s
Q_t total flow-rate through the bed, m^3/s
r_p pore radius, m
R_p radius of porous particle, m
S_c column cross-sectional area, m^2
S_0 cross-sectional area of model porous medium, m^2
$V_{b,i}$ interstitial fluid velocity in column, m/s
$V_{b,sup}$ superficial fluid velocity in column, m/s
v_{DA} diffusion velocity of solute A in the porous medium (porous particle), m/s
$v_{p,i}$ intraparticle interstitial fluid velocity, m/s
$v_{p,sup}$ superficial intraparticle fluid velocity, m/s

Greek symbols
α_1 effective molecular radius of solute A, m
ΔC_A concentration difference of solute A between pore ends, kg/m^3
ε void fraction of bed (bed porosity)
ε_p porosity of the porous medium
ε_t total porosity of the column
μ viscosity of liquid solution, kg/(m·s)
$\varphi(r_p, \alpha_1)$ functional form given in Eq. (8)

Acknowledgements

The authors gratefully acknowledge partial support of this work by Monsanto and the Biochemical Processing Institute of the University of Missouri-Rolla.

References

[1] J.V. Dawkins, L.L. Lloyd, F.P. Warner, J. Chromatogr. 352 (1986) 157.
[2] L.L. Lloyd, F.P. Warner, J. Chromatogr. 512 (1990) 365.
[3] N.B. Afeyan, N.F. Gordon, I. Mazsaroff, L. Varady, S.P. Fulton, Y.B. Yang, F.E. Regnier, J. Chromatogr. 519 (1990) 1.
[4] S.P. Fulton, N.B. Afeyan, N.F. Gordon, F.E. Regnier, J. Chromatogr. 547 (1991) 452.
[5] A.I. Liapis, M.A. McCoy, J. Chromatogr. 599 (1992) 87.
[6] G. Carta, M.E. Gregory, D.J. Kirwan, H.A. Massaldi, Sep. Technol. 2 (1992) 62.
[7] M.A. McCoy, A.I. Liapis, K.K. Unger, J. Chromatogr. 644 (1993) 1.
[8] D.D. Frey, E. Schweinheim, C. Horvath, Biotechnol. Prog. 9 (1993) 273.
[9] G. Carta, A.E. Rodrigues, Chem. Eng. Sci. 48 (1993) 3927.
[10] A.E. Rodriguez, Z.P. Lu, J.M. Loureiro, G. Carta, J. Chromatogr. A 653 (1993) 189.
[11] A.I. Liapis, M.A. McCoy, J. Chromatogr. A 660 (1994) 85.
[12] A.I. Liapis, Math. Modelling and Sci. Computing 1 (1994) 397.
[13] A.I. Liapis, Y. Xu, O.K. Crosser, A. Tongta, J. Chromatogr. A 702 (1995) 45.
[14] G.A. Heeter, A.I. Liapis, J. Chromatogr. A 711 (1995) 3.
[15] Y. Xu, A.I. Liapis, J. Chromatogr. A 724 (1996) 13.
[16] G.A. Heeter, A.I. Liapis, J. Chromatogr. A 734 (1996) 105.

[17] G.A. Heeter, A.I. Liapis, J. Chromatogr. A 743 (1996) 3.
[18] G.A. Heeter, A.I. Liapis, J. Chromatogr. A 760 (1997) 55.
[19] G.A. Heeter, A.I. Liapis, J. Chromatogr. A 761 (1997) 35.
[20] G.A. Heeter, A.I. Liapis, J. Chromatogr. A 776 (1997) 3.
[21] P.-E. Gustavsson, A. Axelsson, P.-O. Larsson, J. Chromatogr. A 795 (1998) 199.
[22] D. Nicolson, J.H. Petropoulos, J. Phys. D. 8 (1975) 1430.
[23] J. Koplik, T.J. Lasseter, Chem. Eng. Commun. 26 (1984) 285.
[24] J. Koplik, S. Redner, D. Wilkinson, Phys. Rev. A 37 (1988) 2619.
[25] S.D. Rege, H.S. Fogler, AIChE J. 34 (1988) 1761.
[26] M. Sahimi, V.L. Jue, Phys. Rev. Letts. 62 (1989) 629.
[27] J.H. Petropoulos, A.I. Liapis, N.P. Kolliopoulos, J.K. Petrou, N.K. Kanellopoulos, Bioseparation 1 (1990) 69.
[28] J.K. Petrou, J.H. Petropoulos, N.K. Kanellopoulos, A.I. Liapis, in A.B. Mersmann, S.E. Scholl (Editors), Proceedings of the Third International Conference on Fundamentals of Adsorption, Engineering Foundation, New York, 1990, p. 679.
[29] A.O. Imdakm, M. Sahimi, Chem. Eng. Sci. 46 (1991) 1977.
[30] R.L. Portsmouth, L.F. Gladden, Chem. Eng. Sci. 46 (1991) 3023.
[31] J.H. Petropoulos, J.K. Petrou, A.I. Liapis, Ind. Eng. Chem. Res. 30 (1991) 1281.
[32] M.P. Hollewand, L.F. Gladden, Chem. Eng. Sci. 47 (1992) 1761.
[33] D. Stauffer, A. Aharony, Introduction to Percolation Theory, Taylor and Francis, London, 2nd ed., 1992.
[34] K.-C. Loh, D.I.C. Wang, J. Chromatogr. A 718 (1995) 239.
[35] W.C. Conner, A.M. Lane, K.M. Ng, M. Goldblatt, J. Catal. 83 (1983) 336.
[36] R. Mann, J.J. Almeida, M.N. Mugerwa, Chem. Eng. Sci. 41 (1986) 2663.
[37] A.I. Liapis, H. Sadikoglu, O.K. Crosser, J. Chromatogr. A, 828 (1998) in press.
[38] K.-C. Loh, Ph.D. Thesis, Department of Chemical Engineering, Massachusetts Institute of Technology, Cambridge, MA, 1995.
[39] J.J. Meyers, Internal Report Number 12, Department of Chemical Engineering, University of Missouri-Rolla, Rolla, MO, 1998.
[40] R.P. Mayer, R.A. Stowe, J. Colloid. Sci. 20 (1965) 893.
[41] D.M. Smith, D.L. Stermer, Powder Technol. 53 (1987) 23.
[42] Z. Dagan, S. Weinbaum, R. Pfeffer, J. Fluid Mech. 115 (1982) 505.
[43] F.A.L. Dullien, Porous Media: Fluid Transport and Pore Structure, Academic Press, New York, 2nd ed., 1992.
[44] S.D. Rege, H.S. Fogler, Chem. Eng. Sci. 42 (1987) 1553.
[45] E.M. Renkin, J. Gen. Physio. 38 (1954) 225.
[46] H. Brenner, L.J. Gaydos, J. Colloid Interface Sci. 58 (1977) 312.
[47] E.A. Mason, R.P. Wendt, E.H. Bresler, J. Membr. Sci. 6 (1980) 283.
[48] N.W. Carlson, J.S. Dranoff, in A.I. Liapis (Editor), Proceedings of the Second International Conference on Fundamentals of Adsorption, Engineering Foundation, New York, 1987, p. 129.